

## Photophysical properties of Sn(IV)tetraphenylporphyrin-pyrene dyad with a $\beta$ -vinyl linker

P. Silviya Reeta<sup>\*a</sup>, Adis Khetubol<sup>a</sup>, Tejaswi Jella<sup>b</sup>, Vladimir Chukharev<sup>a</sup>,  
Fawzi Abou-Chahine<sup>a</sup>, Nikolai V. Tkachenko<sup>a</sup>, L. Giribabu<sup>\*b</sup>  
and Helge Lemmetyinen<sup>\*a</sup>

<sup>a</sup>Department of Chemistry and Bioengineering, Tampere University of Technology, P.O. Box 541,  
FIN-33101 Tampere, Finland

<sup>b</sup>Inorganic & Physical Chemistry Division, CSIR-Indian Institute of Chemical Technology, Uppal Road,  
Tarnaka, Hyderabad 500007, Telangana, India

*Dedicated to Professor Shunichi Fukuzumi on the occasion of his retirement*

Received 30 October 2014

Accepted 25 November 2014

**ABSTRACT:** A Sn(IV)tetraphenylporphyrin (T) has been functionalized with a  $\beta$ -vinyl pyrene (P) and the photophysical properties of the formed dyad (T-P) with its corresponding precursors were studied in three solvents with different polarities using steady-state and time-resolved measurements in ps and fs timescales. When the pyrene moiety is excited at  $\lambda_{ex} = 340$  nm, the fluorescence spectroscopy experiments indicate in all the studied solvents, an efficient quenching of the pyrene emission. When excited at either  $\lambda_{ex} = 340$  nm or  $\lambda_{ex} = 405$  nm, where porphyrin absorbs, a new emissive excited state complex (T-P)\* is observed at wavelengths close to the parent porphyrin emission. The emission is more pronounced in nonpolar hexane showing a mono-exponential decay, but bi-exponential decays are observed in more polar dichloromethane and acetonitrile. When the porphyrin moiety is excited at  $\lambda_{ex} = 425$  nm, the fs transient absorption analysis shows two different intermediate species (~7–11 ps and 80–100 ps) with broad absorption in the near-IR region. This implies either the existence of two different excited conformers (T-P)\*, which decay to the ground state *via* a charge separated state (CSS), or the formation of the (T-P)\* state *via* the second excited state of the porphyrin moiety, yielding first an excited emissive  $\psi$ (T-P)\* state, with a lifetime of 80–100 ps.

**KEYWORDS:** Sn(IV)tetraphenylporphyrin,  $\beta$ -vinyl pyrene donor, optical properties, fs transient absorption, kinetics.

## INTRODUCTION

Porphyrin and their metallo derivatives render as potential chromophores in a wide variety of organo-electronic applications [1–8]. While their close resemblance with the natural photosynthetic reaction center [9–13] represent them as unique model systems to understand the more complex photoinduced electron and energy transfer reactions occurring in nature [7].

Though extensive reports are available describing the intramolecular excitation energy transfer (EET) and photoinduced electron transfer (PET) in a variety of porphyrin-based donor-acceptor (D-A) systems with a donor/acceptor attached either at a peripheral (*-meso* [14–19] or  $\beta$ -pyrrolic [20–24]) or at axial position of resident metallo/metalloid center [27–31], there endures a continual interest in exploring the excited state behavior of such D-A systems. Markedly, functionalizing the pyrrole- $\beta$  position with donors/acceptors has gained special importance due to the favorable in-plane orbital overlap of the peripheral donor with the  $\pi$ -conjugated macrocycle, which sequentially enhances the effective

<sup>†</sup>SPP full member in good standing

\*Correspondence to: Helge Lemmetyinen, email: helge.lemmetyinen@tut.fi, tel: +358 40-581-1347

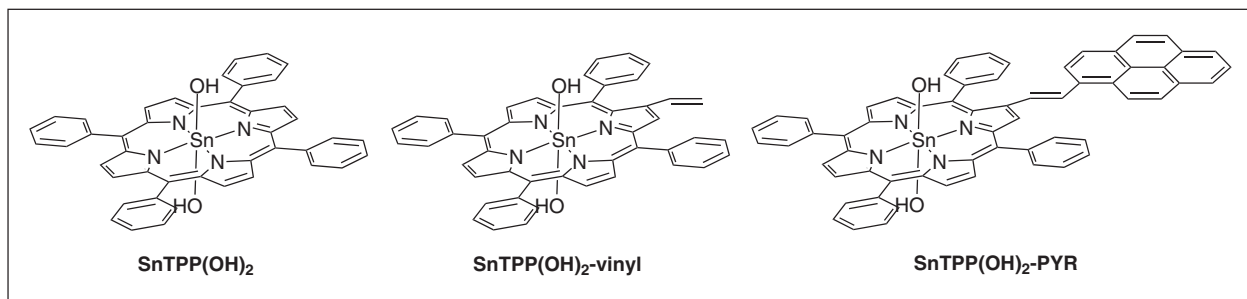


Fig. 1. Molecular structure of the Sn(IV)porphyrin-pyrene dyad and its precursors

electron/energy transfer between the peripheral substitution with the porphyrin ring [20–24].

The fascinating photophysical aspects of Sn(IV) porphyrin supramolecular architectures were investigated previously [29] by employing a wide range of axially ligated donors and acceptors. Recently, we investigated photophysical properties of porphyrin-pyrene dyad in which pyrene is connected at  $\beta$ -pyrrolic position of either a free-base or Zn(II) porphyrin [24]. In this report, the macrocyclic Sn(IV)porphyrin conjugation is extended with a pyrene chromophore *via* a vinylene spacer at the  $\beta$ -pyrrolic position (Fig. 1) and its influence on the structural, redox, and excited state properties of the macrocycle have been dealt in detail using various spectroscopic techniques in the subsequent sections. Further research on axial substitution of the Sn(IV) porphyrin-pyrene dyad with specific acceptor moieties is being continued in our laboratory.

## EXPERIMENTAL

### General

All the reagents and solvents used for the reactions were purchased from Sigma-Aldrich. The solvents utilized for the electrochemical and spectral analysis were further purified by following standard procedures [32]. Moisture sensitive reactions were performed under an inert atmosphere of nitrogen. Chromatographic purifications were performed using Silica gel (60–120 mesh) and neutral or basic alumina (activity grade I).

The UV-visible spectra were recorded on a Shimadzu (Model UV-3600) spectrophotometer using  $1 \times 10^{-6}$  M concentrations. The steady-state fluorescence measurements were performed on a Fluorolog-3 spectrofluorometer (Spex Model, JobinYvon). The concentration of the solutions were maintained constantly at OD < 0.1 for all the compounds in order to eliminate the possibility of quenching caused by the aggregation and to minimize nonlinear absorption and re-absorption effects.

The time correlated single photon counting (TCSPC) method was used for measuring the fluorescence lifetime of the molecules in their excited state. The base (PicoQuant

GmbH) system consisted of PicoHarp-200 controller, a PDL-800-B driver and pulsed LED (PLS-8-2-295) and pulsed diode (LDH-P-C-405B) exciting samples at 340 and 405 nm, respectively. The detection part consisted of micro-channel photomultiplier tube (R3809u-50 Hamamatsu) coupled with a monochromator. The time resolution of the system was roughly 300 and 60 ps with excitation at 340 and 405 nm, respectively. The data were analyzed using a freely available software package Decfit. The quality of the fit was ascertained from the  $\chi^2$  values and the distribution of residuals. Differential pulse voltammetric (DPV) technique was performed using a PC-controlled electrochemical analyzer (CH instrument model CHI620C) using Ferrocene as the standard and 0.1 M TBAP (*vs.*) SCE under standard experimental conditions.

The fluorescence decay associated spectra (DAS) were obtained by global fitting of the fluorescence decays, measured at every 10 nm over the region of the emission spectrum (550–800 nm) ( $\chi^2 \sim 1.1$ ), at a fixed excitation intensity and measurement time. The relative amplitudes of the decay components were further corrected by a function corresponding to the detector sensitivity [33].

Ultrafast fluorescence decays were measured using an up-conversion method described elsewhere [34] with a temporal resolution of  $\sim 150$  fs. In brief, fundamental pulses of 840 nm produced by a Ti:Sapphire laser (TiF50, CDP-Avesta) at 80 MHz repetition rate were split into two beams. One portion underwent second harmonic generation to excite the sample at 420 nm, generating emission. The second portion of the fundamental pulse beam was passed to a delay line and then mixed with the emission to achieve frequency up-conversion. The resulting UV photons were detected by a photon counting photomultiplier coupled with a monochromator with a typical averaging of 10 s at each delay time.

For transient absorption measurements, a sub-picosecond resolution setup was used and described in detail elsewhere [34, 35]. Briefly, 800 nm laser pulses at 1 kHz repetition rate were generated by a Ti:Sapphire laser system (Libra F, Coherent Inc.). The fundamental pulses were split into two beams; one pump beam was guided through an optical parametric amplifier (Topas C, Light Conversion Ltd.) to generate the excitation pulses

at 340 and 425 nm. The pump beam and the rest of fundamental were delivered to a pump-probe measurement system (ExciPro, CDP Inc.). The system generated a white light continuum (WLC) from the 800 nm beam which was used as a probe pulse. The probe was guided through a delay line with a moving right angle reflector that changed the optical path length of the probe with respect to the pump beam. The maximum time scale available to monitor absorption changes was *ca.* 6 ns. The probe pulse was split into two to obtain signal and reference beams that both passed through the sample. The signal beam was overlapped with the pump beam while the reference beam was not. The excitation was modulated by a chopper synchronized excitation pulses to detect probe pulse spectra with and without the excitation and to calculate differential transient absorbance for each excitation pulse. Measurements were recorded with a 10 s average for each delay time, *i.e.* averaging 10000 excitation shots. The spectra were acquired in two ranges, 460–780 nm and 850–1050 nm. The measurements around fundamental wavelength, 800 nm, were unreliable since the continuum was very uneven close to the fundamental.

The raw data were fit globally by a sum of exponents to perform data analysis, a procedure which has been described in more detail previously [34]. Briefly, the number of exponents needed for a reasonable fit quality yielded the number of transient species in the photo-induced processes. The rate constants for the formation or relaxation of transient species can be calculated from the respective lifetimes of each component. The results of the fits are presented as decay component spectra with the amplitudes of the exponents plotted as functions of wavelength.

### Synthesis

The 5,10,15,20-tetraphenylporphyrinato tin(IV) [SnTPP(OH)<sub>2</sub>] [36], 2-vinyl-5,10,15,20-tetraphenylporphyrinato tin(IV) [SnTPP(OH)<sub>2</sub>-vinyl] [37], and 2-pyrenyl-5,10,15,20-tetraphenylporphyrinato tin(IV) [SnTPP(OH)<sub>2</sub>-PYR] [20, 22] were synthesized by following the literature reported procedures. The synthetic details are presented in the experimental procedure below.

### General procedure for the synthesis of dihydroxy Sn(IV)porphyrins

The dihydroxy tin(IV) porphyrins were synthesized by refluxing the corresponding free-base porphyrin (2.0 g, 3 mM, for representative H<sub>2</sub>TPP) and SnCl<sub>2</sub>·2H<sub>2</sub>O (3.0 g, 13 mM) dissolved in 50 mL of pyridine for 2 h. Then the mixture was cooled and pyridine was removed under reduced pressure. The solid obtained was dissolved in CHCl<sub>3</sub> and washed several times with water. The organic layer was dried by passing through anhydrous Na<sub>2</sub>SO<sub>4</sub> and chromatographed over basic alumina. Elution with CHCl<sub>3</sub>/CH<sub>3</sub>OH (98:2 V/V) gave the corresponding dichloro tin(IV) porphyrins. Yield upto 95%.

A 10% aqueous NaOH solution was added to the CHCl<sub>3</sub> solution of the corresponding dichloro Sn(IV) porphyrin and the mixture was stirred at room temperature for 2 h. The organic layer was separated and dried to get violet solid of the corresponding dihydroxy Sn(IV) porphyrin, which were recrystallized from CH<sub>2</sub>Cl<sub>2</sub>-hexane. Yield upto 90%.

**SnTPP(OH)<sub>2</sub>.** Yield 90%. ESI-MS: *m/z* C<sub>44</sub>H<sub>30</sub>N<sub>4</sub>O<sub>2</sub>Sn, (765.44): [M + H<sup>+</sup>] 766 (85%). <sup>1</sup>H NMR (CDCl<sub>3</sub>): δ, ppm 9.15 (s, 8H), 8.18 (m, 8H), 7.80 (m, 12H).

**SnTPP(OH)<sub>2</sub>-vinyl.** Yield 87%. ESI-MS: *m/z* C<sub>46</sub>H<sub>32</sub>N<sub>4</sub>O<sub>2</sub>Sn, (791.50): [M + 2H<sup>+</sup>] 793 (100%). <sup>1</sup>H NMR (CDCl<sub>3</sub>): δ, ppm 8.75 (multiplet, 7H), 8.15 (m, 8H), 7.75 (multiplet, 12H), 6.49 (dd, 1H, *J* = 1.0 Hz, *J* = 10.8 Hz, *J* = 17.1 Hz), 5.90 (dd, 1H, *J* = 2.0 Hz, *J* = 17.1 Hz), 5.15 (dd, 1H, *J* = 2.4 Hz, *J* = 10.8 Hz).

**SnTPP(OH)<sub>2</sub>-PYR.** Yield 90%. ESI-MS: *m/z* C<sub>62</sub>H<sub>40</sub>N<sub>4</sub>O<sub>2</sub>Sn, (991.44): [M + H<sup>+</sup>] 991 (50%). <sup>1</sup>H NMR (CDCl<sub>3</sub>): δ, ppm 9.45 (s, 1H), 9.11 (m, 6H), 8.56 (s, 1H), 8.38 (m, 8H), 8.21 (m, 4H), 8.12 (s, 2H), 8.01 (m, 2H), 7.86 (m, 12H), 7.32 (d, 1H, *J* = 15.9), 7.16 (d, 1H, *J* = 15.9 Hz).

## RESULTS AND DISCUSSION

Preliminary characterization of the molecules synthesized was performed with ESI-MS, <sup>1</sup>H NMR, and UV-visible absorption spectroscopy. Mass spectral data *m/z*, (Rel.Int.%) of [SnTPP(OH)<sub>2</sub>-vinyl]: [M + 2H]<sup>+</sup>, 793 (100) and [SnTPP(OH)<sub>2</sub>-PYR]: [M + H]<sup>+</sup>, 991 (50) and the corresponding <sup>1</sup>H NMR spectra recorded in CDCl<sub>3</sub> were shown in supplementary material (Fig. S1 to S3) and the chemical shift data in δ, ppm using tetramethylsilane (TMS) as the internal standard was summarized in the experimental section. Both the molecules [SnTPP(OH)<sub>2</sub>-vinyl] and [SnTPP(OH)<sub>2</sub>-PYR] displayed the characteristic β-pyrrolic and *meso*-proton resonance positions of corresponding SnTPP(OH)<sub>2</sub> precursor. Resonance due to –CH=CH<sub>2</sub> in [SnTPP(OH)<sub>2</sub>-vinyl] appear at δ 6.49 (dd, 1H, *J* = 1.0 Hz, *J* = 10.8 Hz, *J* = 17.1 Hz), 5.90 (dd, 1H, *J* = 2.0 Hz, *J* = 17.1 Hz), 5.15 (dd, 1H, *J* = 2.4 Hz, *J* = 10.8 Hz). In [SnTPP(OH)<sub>2</sub>-PYR], the pyrene protons appear as more overlapping peaks along with the signals of porphyrin-*meso* protons in the aromatic region while the two vinylic protons appear as doublets at δ 7.32 (d, 1H, *J* = 15.9) and 7.16 (d, 1H, *J* = 15.9 Hz).

### Optical properties

The UV-visible absorption spectrum of the dyad is compared with those of its precursors in Fig. 2 and the data are summarized in Table 1. The absorption of pyrene is mainly at the 300–350 nm region. For SnTPP(OH)<sub>2</sub>-vinyl and SnTPP(OH)<sub>2</sub>, the absorption bands are displayed at the very same wavelength regions with intense Soret bands appearing at around 425 nm and two less intense Q-bands around 500 to 620 nm region.

The absorption peaks are slightly broadened and red shifted by ~5–6 nm for the SnTPP(OH)<sub>2</sub>-PYR dyad

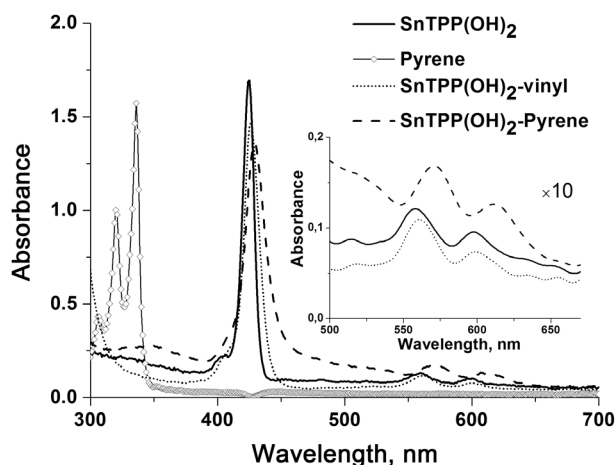


Fig. 2. UV-visible absorption spectra of pyrene and the studied Sn(IV)porphyrin derivatives in  $\text{CH}_2\text{Cl}_2$

Table 1. UV-visible data ( $1 \times 10^{-6}$  M for Soret and  $1 \times 10^{-3}$  M for Q-bands)

Compound	Absorption, $\lambda_{\text{max}}$ , nm ( $\log \epsilon$ , $\text{M}^{-1} \cdot \text{cm}^{-1}$ ) <sup>a</sup>					
	Porphyrin bands			Pyrene bands		
<b>SnTPP(OH)<sub>2</sub></b>	425 (5.07)	560 (4.10)	600 (3.85)	—		
<b>SnTPP(OH)<sub>2</sub>-vinyl</b>	426 (5.01)	562 (4.05)	601 (3.05)	—		
<b>SnTPP(OH)<sub>2</sub>-PYR</b>	426 (5.06)	557 (4.03)	597 (3.54)	239 (3.30)	290 (4.30)	347 (4.39)
<b>Pyrene</b>	—			290 (4.55)	333 (4.39)	376 (4.34)

<sup>a</sup>Solvent  $\text{CH}_2\text{Cl}_2$ , error limits:  $\lambda_{\text{max}}$ ,  $\pm 1$  nm,  $\log \epsilon$ ,  $\pm 10\%$ .

due to the presence of extended conjugation *via* the vinyl spacer. The results indicate a weak ground state interaction between the porphyrin and pyrene moieties in **SnTPP(OH)<sub>2</sub>-PYR**.

### Electrochemical properties

The redox curves of the reported Sn(IV)porphyrins with their corresponding precursors were measured by differential pulse voltammetry with  $\text{CH}_2\text{Cl}_2$  solvent and 0.1 M TBAP as supporting electrolyte and the data are summarized in supplementary material (Table S1 and Fig. S5). Figure S5 and data in Table S1 indicate that the dyad shows up to two reduction and three oxidation peaks under the experimental conditions employed in this study. Wave analysis suggested that, in general, while the first two reduction steps and the first two oxidation steps are reversible ( $i_{\text{pc}}/i_{\text{pa}} = 0.9\text{--}1.0$ ) and diffusion-controlled ( $i_{\text{pc}}/\nu^{1/2} = \text{constant}$  in the scan rate ( $\nu$ ) range 50–500 mV/s) one-electron transfer ( $\Delta E_p = 60\text{--}70$  mV;

$\Delta E_p = 65 \pm 3$  mV for ferrocenium/ferrocene couple) reactions. The peaks occurring at anodic potentials are ascribed to successive one-electron oxidations of the porphyrin parts of **SnTPP(OH)<sub>2</sub>/SnTPP(OH)<sub>2</sub>-PYR**. As seen in Fig. S5, the pyrene redox potential appears as overlapped peaks in **SnTPP(OH)<sub>2</sub>-PYR** compared to the precursor **SnTPP(OH)<sub>2</sub>**. Quite interestingly, when appended with peripheral pyrene (**SnTPP(OH)<sub>2</sub>-PYR**), the first oxidation potential of porphyrin, shows a cathodic shift by nearly 80 mV compared to its precursor **SnTPP(OH)<sub>2</sub>**. This observation accounts for the influence of attaching a peripheral electron donating pyrene in **SnTPP(OH)<sub>2</sub>-PYR** on the redox properties of Sn(IV)porphyrins.

The spectroscopic and electrochemical features of the Sn(IV)porphyrin-pyrene dyad described above suggest that in the ground state, an electronic communication between the porphyrin and pyrene chromophores, though not significant, but could not be completely ruled out. Nevertheless, the excited state properties of individual chromophores could be more deeply exploited by selective excitation of the individual chromophore units.

### Fluorescence quantum yields

The emission spectra of the Sn(IV)porphyrin precursors and dyads were measured in different solvents with increasing polarity, in hexane (Hex), dichloromethane (DCM), and acetonitrile (AcCN). The recorded emission spectra are displayed in Figs 3 and 4, and the data are summarized in Table 2. The fluorescence quantum yields of the reported compounds were calculated with reference to ZnTPP ( $\phi = 0.036$  in  $\text{CH}_2\text{Cl}_2$ ) [38]. The efficiency of fluorescence quenching was measured by employing Equation 1;

$$Q = \frac{\Phi(D) - \Phi(DA)}{\Phi(D)} \quad (1)$$

where  $\phi(D)$  refers to the fluorescence quantum yield of pyrene or **SnTPP(OH)<sub>2</sub>** whereas  $\phi(DA)$  refers to the quantum yield of **SnTPP(OH)<sub>2</sub>-PYR**.

The emission measurements of the precursor porphyrin were performed at  $\lambda_{\text{ex}} = 425$  nm while the dyad molecule was excited at two different wavelengths, *i.e.*  $\lambda_{\text{ex}} = 340$  nm or 425 nm, where the individual subunits pyrene and porphyrin, respectively, absorb predominantly. Considering the dyad molecule, the peripheral pyrene emission ( $\lambda_{\text{em}} = 350\text{--}500$  nm) overlaps with the porphyrin absorption maximum ( $\lambda_{\text{abs}} = 420$  nm) as shown in Fig. S4, which shows the possible occurrence of the energy transfer from the pyrene to the Sn(IV)porphyrin moiety, which is supported by the efficient quenching of pyrene emission (Fig. 3) upto 98% in the dyad at  $\lambda_{\text{ex}} = 340$  nm. This is also supported by the spectral overlap of the excitation spectra of the dyad with its UV-visible absorption spectra in Hex and AcCN (Figs S6 and S7). More importantly, at

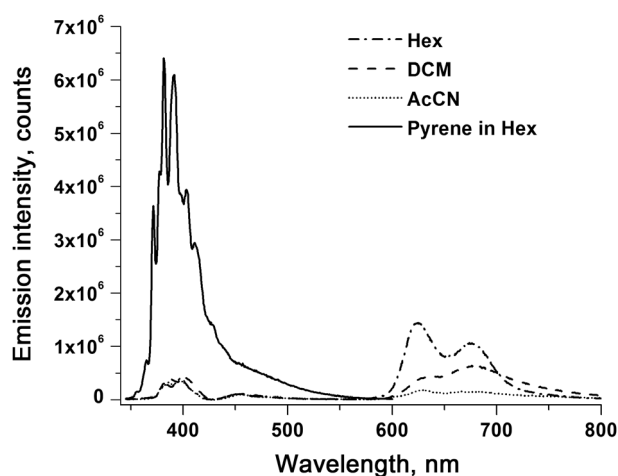


Fig. 3. Fluorescence spectra of pyrene in hexane and  $\text{SnTPP(OH)}_2\text{-PYR}$  in three different solvents.  $\lambda_{\text{ex}} = 340 \text{ nm}$

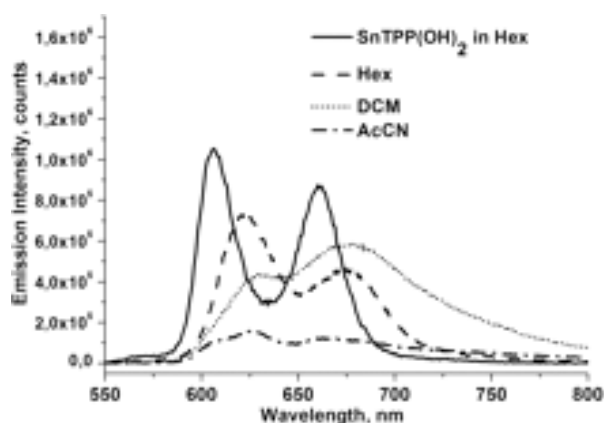


Fig. 4. Fluorescence spectra of  $\text{SnTPP(OH)}_2$  in Hex and  $\text{SnTPP(OH)}_2\text{-PYR}$  in Hex, DCM, and AcCN.  $\lambda_{\text{ex}} = 425 \text{ nm}$

600–750 nm the emission is enhanced with a variation in the intensity ratios accompanied with pronounced broadening and red-shifted maxima compared to that of the  $\text{SnTPP(OH)}_2$  emission (Fig. 3). A similar trend is also observed when the porphyrin chromophore was excited at  $\lambda_{\text{ex}} = 425 \text{ nm}$  (Fig. 4).

Thus, irrespective of the chromophore being excited the dyad shows distinct emission features, which could be possibly due to the formation of an intermediate species, which does not exactly have the emission properties of the neat porphyrin moiety, but is also influenced by the pyrene, covalently linked to it by a double bond. This new intramolecular emissive transient state is a noticeable interesting phenomena in this report. The occurrence of this intermediate species is investigated by the time-resolved measurements at ps and fs time scales, the details of which will be described in the subsequent sections.

### Time-resolved fluorescence experiments

As evidenced from the fluorescence quantum yield (QY) data, a relatively efficient quenching of pyrene monomer emission possibly due to energy transfer, was observed in the  $\text{SnTPP(OH)}_2\text{-PYR}$ . This leads to the formation of a “new emission band” at a longer wavelength, which is no longer characteristic of the pyrene monomer. This new emission band reflects the formation of new excited state which combines properties of both pyrene and porphyrin monomers and could be described as an intramolecular transient state with dual fluorescence properties (see Figs 3 and 4).

To gain further insight of the intramolecular photophysical processes between the pyrene and porphyrin moieties in the dyad, time-correlated single photon counting (TCSPC) experiments were performed

Table 2. Fluorescence data<sup>a</sup> of the studied compounds

Compound	$\lambda_{\text{em}}, \text{nm} (\phi, \%Q^b)$					
	Hexane		$\text{CH}_2\text{Cl}_2$		$\text{CH}_3\text{CN}$	
	$\lambda_{\text{ex}} = 425 \text{ nm}$			$\lambda_{\text{ex}} = 340 \text{ nm}$		
$\text{SnTPP(OH)}_2$	605, 669 (0.043)	605, 661 (0.048)	604, 659 (0.066)			
$\text{SnTPP(OH)}_2\text{-Vinyl}$	606, 661 (0.037)	605, 661 (0.040)	606, 660 (0.045)			
$\text{SnTPP(OH)}_2\text{-PYR}$	630, 679 (0.056)	622, 674 (0.039)	626, 664 (0.020)	383, 394, 456 (0.001, 95)	386, 397, 456 (0.002, 98)	385, 397, 455 (0.001, 98)
				624, 676 (0.083)	637, 677 (0.077)	630, 673 (0.023)
<b>Pyrene</b>	—	—	—	381, 391, 403 (0.021)	372, 383, 392 (0.087)	372, 382, 392 (0.047)

<sup>a</sup>Error limits:  $\lambda_{\text{ex}}, \pm 2 \text{ nm}$ ,  $\phi \pm 10\%$ . <sup>b</sup> $Q$  is defined in Equation 1 (see text).

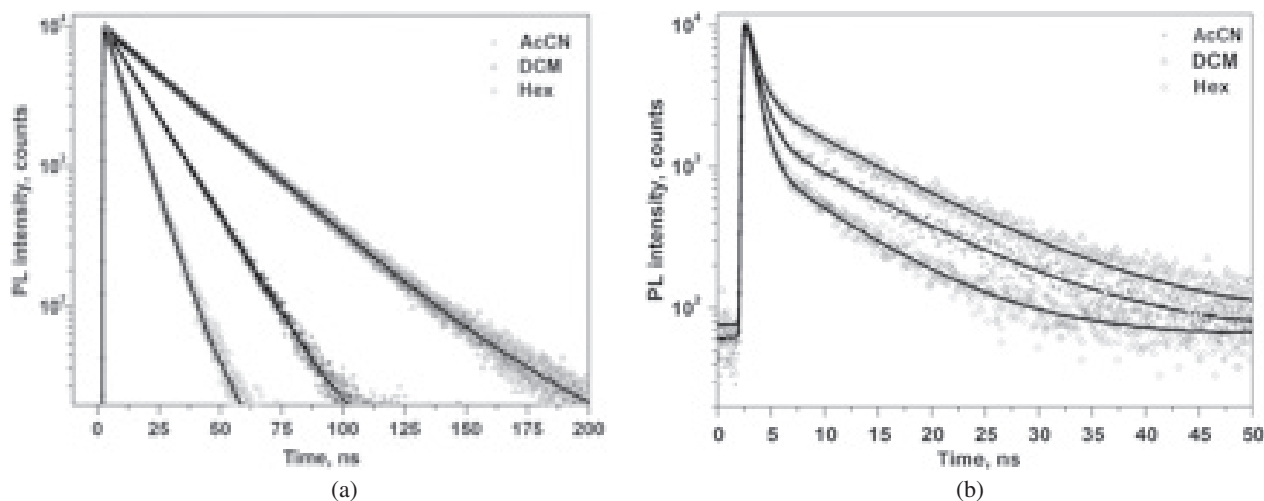


**Fig. 5.** Fluorescence decays of (a) **pyrene** and (b) the **SnTPP(OH)<sub>2</sub>-PYR** in Hex, DCM, and AcCN.  $\lambda_{\text{ex}} = 340$  nm and  $\lambda_{\text{em}} = 385$  nm

in three different solvents with varied static dielectric constants. First, we collected the fluorescence decays of the solutions of the dyad and compared them with those of the corresponding reference compounds, *i.e.* **pyrene** and **SnTPP(OH)<sub>2</sub>** (Figs 5 and 6) and **SnTPP(OH)<sub>2</sub>-vinyl** (Fig. S8). Each sample was excited either at 340 nm (pyrene absorption) or at 405 nm (porphyrin absorption) and the decay times were measured at their corresponding emission maxima in three different solvents. The corresponding decay curves are shown in Figs 5 and 6 and the data are summarized in Tables 3 and 4 (complete data in Table S2 of supplementary material).

From Fig. 5 and Table 3, when excited at  $\lambda_{\text{ex}} = 340$  nm and monitored the pyrene emission at 385 nm in both polar and nonpolar solvents, the decays of the dyad are bi-exponential and the fluorescence lifetimes shorter than that for the pyrene monomer. The shorter ( $\sim 1$  ns) decay component, contributes 75–91% to the fluorescence.

The decreased lifetimes correspond to efficient excitation energy transfer (EET) from pyrene  $\rightarrow$  porphyrin. Moreover, the quenching is more efficient in the nonpolar solvent (hexane) where the larger contribution (91%) of

this component is observed. The quenching rate constants were calculated using Equation 2.

$$k_q = \frac{1}{\tau_f^0} \left( \frac{\Phi_f^0}{\tau_f k_f} - 1 \right) = \frac{1}{\tau_f} - \frac{1}{\tau_f^0} \quad (2)$$

Here  $\Phi_f^0$  is the fluorescence quantum yield of the donor in the absence of acceptor.  $k_f$  is the fluorescence decay rate constant of the donor.  $\tau_f$  and  $\tau_f^0$  are the decay times of the donor in the presence and absence of the acceptor, respectively. The time  $\tau_f$  corresponds to the lifetime of the shorter living component observed for the dyad, while  $\tau_f^0$  corresponds to the lifetime of the single exponential decay observed for the monomer. The calculated rate constants are summarized in Table 3.

The results in Table 3 are in a relatively good agreement with the quantum yield data collected from the steady-state emission experiment (Table 2). Furthermore, the decay of the dyad emission by two different time constants might be due to an equilibrium formed between the excited monomer in the dyad and the excited emissive state, as will be discussed later. On the other hand it

**Table 3.** Fluorescence decay times, amplitudes and quenching rate constants ( $k_q$ ,  $\text{s}^{-1}$ )<sup>‡</sup> at  $\lambda_{\text{ex}} = 340$  nm and  $\lambda_{\text{em}} = 385$  nm analyzed from the fluorescence decay curves in Fig. 5

Compound	Solvent	$\tau_1$ , ns	$\tau_2$ , ns	$k_q$ , $\text{s}^{-1}$
<b>Pyrene</b>	Hexane	8.20 (100%)	—	—
	DCM	28.81 (100%)	—	—
	AcCN	15.12 (100%)	—	—
<b>SnTPP(OH)<sub>2</sub>-PYR</b>	Hexane	0.77 (90.8%)	7.59 (9.2%)	$1.18 \times 10^9$
	DCM	1.12 (75.3%)	10.91 (24.7%)	$0.86 \times 10^9$
	AcCN	0.94 (86.3%)	10.27 (13.7%)	$1.00 \times 10^9$

$k_q$ <sup>‡</sup> is the quenching rate constant of the pyrene emission observed for the **SnTPP(OH)<sub>2</sub>-PYR** dyad calculated according to Equation 2. Error limits of  $\tau$  and  $k_q \sim 10\%$ . Values in parenthesis are the relative amplitudes of corresponding decay components.

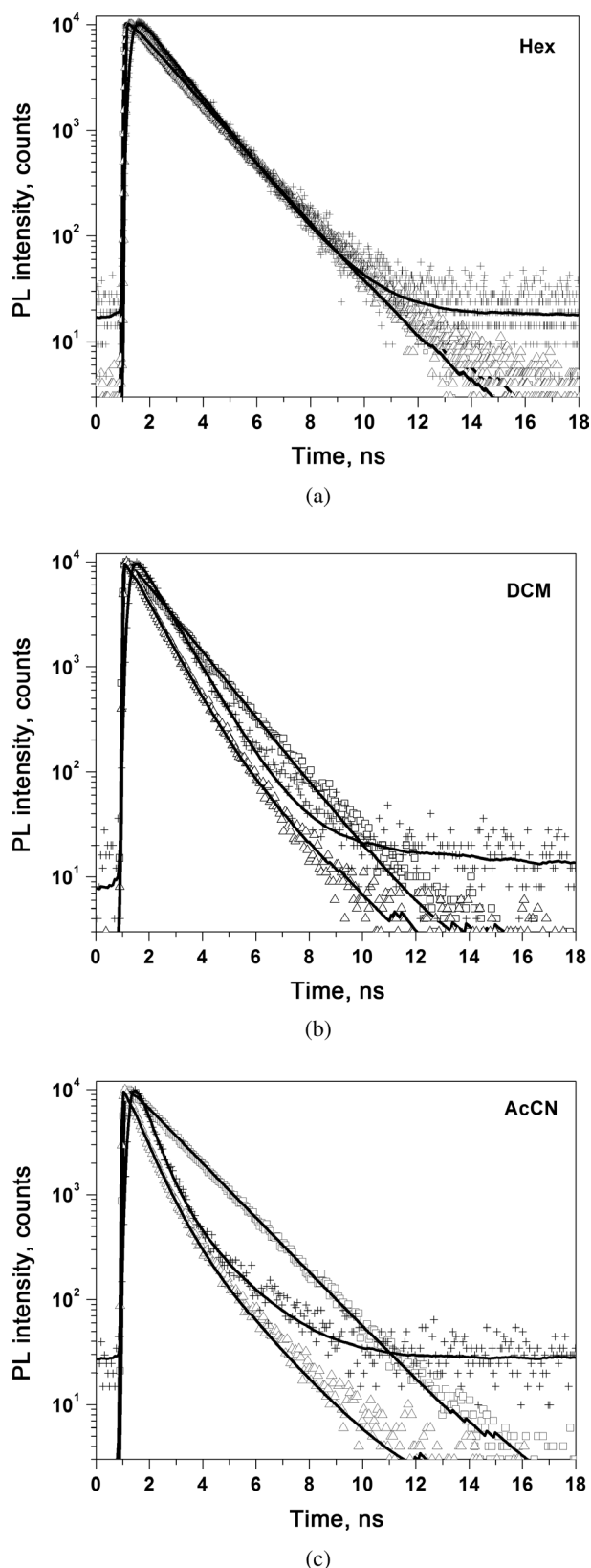


**Fig. 6.** Fluorescence decays of  $\text{SnTPP(OH)}_2$  ( $\square\square\square$ ,  $\lambda_{\text{ex}} = 405$  nm,  $\lambda_{\text{em}} = 650$  nm) and  $\text{SnTPP(OH)}_2\text{-PYR}$  ( $\triangle\triangle\triangle$ ,  $\lambda_{\text{ex}} = 405$  nm,  $\lambda_{\text{em}} = 675$  nm) and  $\text{SnTPP(OH)}_2\text{-PYR}$  ( $+++$ ,  $\lambda_{\text{ex}} = 340$  nm,  $\lambda_{\text{em}} = 675$  nm) in (a) Hex, (b) DCM, and (c) AcCN

might imply the formation of two distinguished excited states, which decay to the ground state with different time constants, which is probably caused by a change of the molecular conformation [18].

From Fig. 6 and Table 4, when excited at  $\lambda_{\text{ex}} = 405$  nm, and monitored at the porphyrin emission maxima, 650 nm–675 nm, the decay curves of the dyad were bi-exponential in DCM and AcCN, with the shorter lifetime component having the major amplitude. Whereas in hexane the decay was mono-exponential. Thus, in DCM and AcCN, irrespective of the wavelength of the chromophore being excited, *i.e.*  $\lambda_{\text{ex}} = 340$  nm (where the absorption ratio is about 1.7:1 for pyrene:porphyrin) or 405 nm (which excites selectively porphyrin chromophore), the fluorescence decays can be analyzed as a sum of two exponentials. The decay times and amplitudes are presented in Table 4.

Comparing the lifetimes in Tables 3 and 4, one can observe that monitoring either at 385 nm (pyrene emission) or at  $>650$  nm (porphyrin emission), the decays for  $\text{SnTPP(OH)}_2\text{-PYR}$  are bi-exponential in all solvents, when monitored at the pyrene or porphyrin emission wavelengths, except the porphyrin emissions in hexane. In the case of nonpolar hexane, the decay is mono-exponential and the lifetime is the same as that of  $\text{SnTPP(OH)}_2$ . The results suggest that the final excited state of the dyad combines the properties of both pyrene and porphyrin monomers and can no longer be considered as individual monomers. The relative amplitudes of the decay components however are slightly different at different excitation wavelengths. Especially the longer decay times in the later case ( $\lambda_{\text{ex}} = 405$  nm) are considerably shorter.

For the emission at wavelength  $>410$  nm the time constants are very close to each other regardless of the chromophore being excited, *i.e.* in pyrene or porphyrin absorption band. This could be attributed to the stabilization of only one intermediate species in nonpolar hexane, whereas in polar solvents, there is a probability for the formation of different excited states, *e.g.* a charge separated or a conformeric state, which both could account for the two decay components.

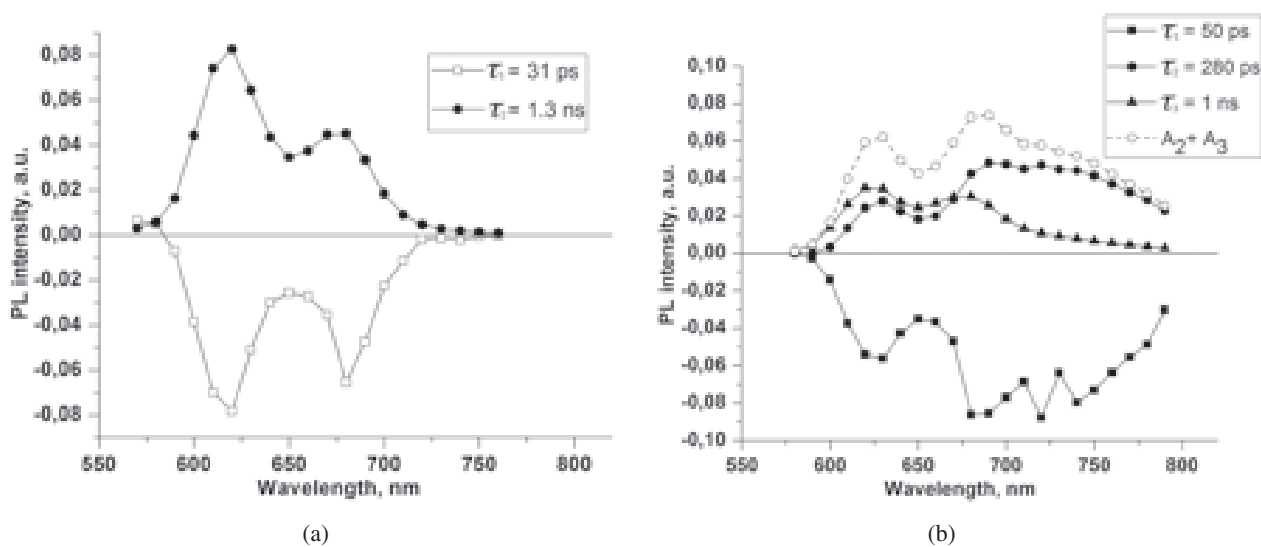
### Decay associated spectra

As mentioned above the final excited state of the dyad combines properties of both the chromophores and can no longer be considered as pyrene (**P**) or porphyrin (**T**) moieties individually. The relative amplitudes of the decay components are slightly different at different excitation wavelengths. Namely, the shorter living component has little larger contribution when excitation occurred at 340 nm, while the longer living component has little larger contribution when excitation occurred at 405 nm. The decay of the  $\text{SnTPP(OH)}_2\text{-PYR}$  (T-P) dyad emission by two different time constants might be due, on

**Table 4.** Fluorescence decay times, amplitudes and quenching rate constant ( $k_q$ ,  $s^{-1}$ )<sup>‡</sup> at  $\lambda_{exc}$  = 340 or 405 nm, and  $\lambda_{em}$  at porphyrin emission maxima analyzed from the fluorescence decay curve in Fig. 6

Compound	Solvent	$\lambda_{exc}$ , nm	$\lambda_{em}$ , nm	$\tau_1$ , ns	$\tau_2$ , ns	$k_q$ , $s^{-1}$
<b>SnTPP(OH)<sub>2</sub></b>	Hexane	405	650	1.54 (100)	—	—
	DCM	—	—	1.39 (100)	—	—
	AcCN	—	—	1.67 (100)	—	—
<b>SnTPP(OH)<sub>2</sub>-PYR</b>	Hexane	340	675	1.36 (100)	—	No quenching
	—	405	675	1.52 (100)	—	No quenching
	DCM	340	675	0.91 (88.8)	2.07 (11.2)	$0.38 \times 10^9$
	—	405	675	0.63 (52.5)	1.22 (47.5)	$0.87 \times 10^9$
	AcCN	340	675	0.50 (84.5)	1.67 (15.5)	$1.40 \times 10^9$
	—	405	675	0.57 (87.4)	1.65 (12.6)	$1.15 \times 10^9$

$k_q$ <sup>‡</sup> is the quenching rate constant of the pyrene emission observed for the **SnTPP(OH)<sub>2</sub>-PYR** dyad calculated according to Equation 2. Error limits of  $\tau$  and  $k_q \sim 10\%$ . Values in parenthesis are the relative amplitudes of corresponding decay components.

**Fig. 7.** The fluorescence decay associated spectra of T-P dyad in Hex (a) and in AcCN (b) at 405 nm excitation. The time constants with negative amplitudes, about 30 and 50 ps, are on the limit of the time resolution of the instruments

one hand, to an equilibrium formed between the excited monomer in the dyad and the excited emissive state. This could be especially in the case of pyrene emission (Table 3). On the other hand it might imply the formation of two distinguished excited states, which decay to the ground state with different time constants, which could be caused either by a change of the molecular conformation [18] or by reactions of different excited state, *e.g.* the first and second excited state.

Since the two distinguished decay components were observed from the dyad in the polar solvents, it is worth to further investigate how these species contribute over the range of the emission band. Hence the fluorescence decay associated spectra (DAS) of the T-P dyad in hexane and AcCN were measured.

The results of DAS measurements are shown in Fig. 7. Two different components are formed in times of few tens of picosecond (31 and 50 ps) and decay mono-exponentially (1.3 ns) in hexane, whereas bi-exponentially (280 ps and 1 ns) in AcCN. Although the formation times of 30–50 ps are on the limit of the time resolution of TCSPC-method, and thus that of the DAS-method, these components could imply a formation of the (T-P)\* state from the primary excited T\*-P state.

### Fluorescence up-conversion experiments

The fluorescence up-conversion lifetime measurements for T-P dyad in AcCN gave decay curves with three major decay components; a fast component, 10 ps, a

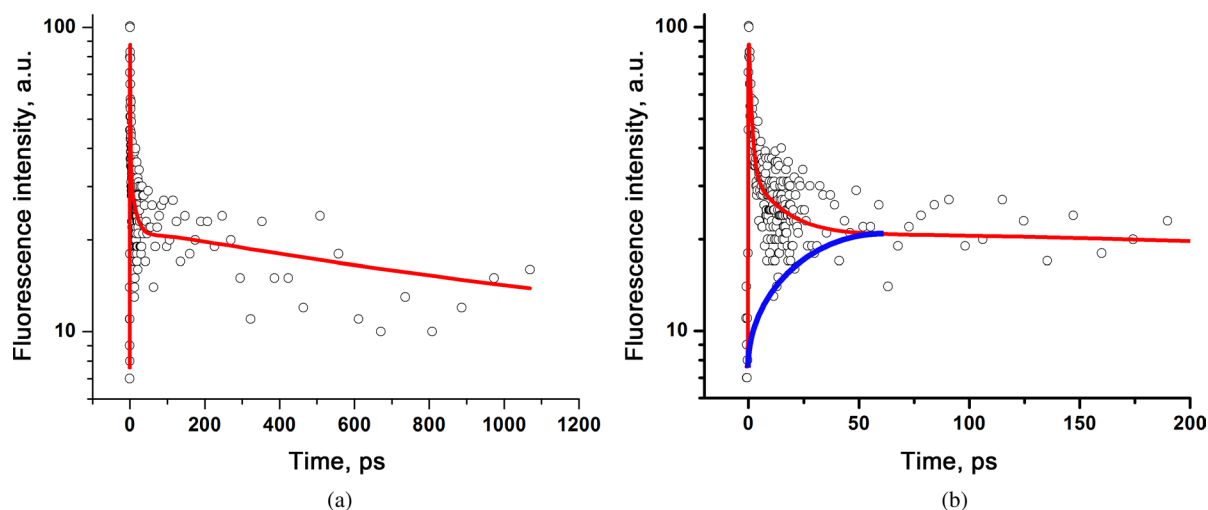


**Fig. 8.** The fluorescence up-conversion decay curves of T-P dyad in Hex, excited at 420 nm and monitored at 615 nm, with time windows of (a) 1.1 ns and (b) 200 ps. The decay can be analysed as three-exponential, yielding  $\tau_1 = 10$  ps (84%),  $\tau_2 = 25$  ps (-36%), and  $\tau_3 = 1.3$  ns (52%). The growing of 25 ps component is indicated by the blue curve

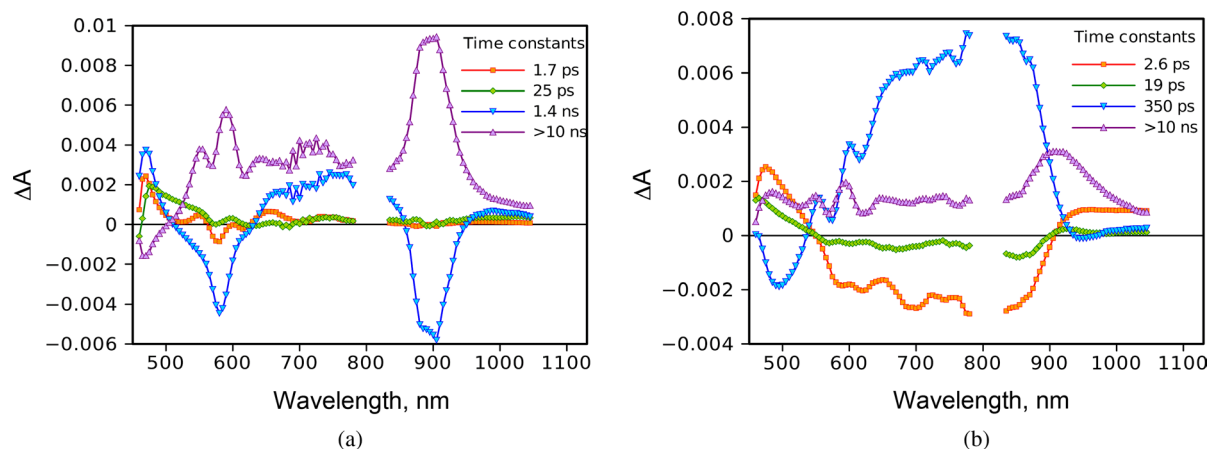


**Fig. 9.** Transient component spectra of T-P dyad in Hex (a) and AcCN (b) at  $\lambda_{\text{ex}} = 340$  nm

longer-living component, about 1.3 ns, and a component with a negative amplitude, 25 ps (see Fig. 8 and its caption). The determined lifetimes coincide reasonably well with those obtained by the DAS-method. The very fast component (10 ps, in up-conversion) could be the fluorescence lifetime of the T moiety, while the longer-living (about 1.3 ns) component should correspond to the emission of the (T-P)\* complex. Moreover this 1.3 ns component fits very well with the single-exponential decay of the dyad in hexane, observed in TCSPC experiment. The additional intermediate component with a negative amplitude and lifetime of ~25 ps resembles the 30–50 ps components observed in the DAS experiments and corresponds to the formation of (T-P)\*.

### Ultra-fast pump-probe experiments

The transient absorption behavior of T-P compound was studied by the femtosecond pump-probe method

with excitation both at 340 nm (pyrene absorption) and at 425 nm (porphyrin absorption). The transient absorption component spectra, at 340 nm excitation, in hexane and acetonitrile are shown in Fig. 9.

In hexane (Fig. 9(a)) a ~2 ps component corresponds to the singlet excited state of the pyrene moiety. This is followed by a 25 ps component, and a formation of the excited dyad, (T-P)\*. This fits very well with the 25 ps component observed in the fluorescence up-conversion experiment. (T-P)\* has a broad absorption from 620 nm to 850 nm, with a lifetime of 1.4 ns. These results also coincide well with fluorescence up-conversion and TCSPC results. The negative bands (1.4 ns) at 500–620 nm and 860–940 nm describe the formation of the final transient state, with lifetime longer than 6 ns, the upper limit of the instrument, and a broad intense absorption from 500 to 950 nm, with two main maxima. This state could be cation radical (at shorter wavelength) of SnTPP and anion radical (at longer wavelength) of pyrene moieties.

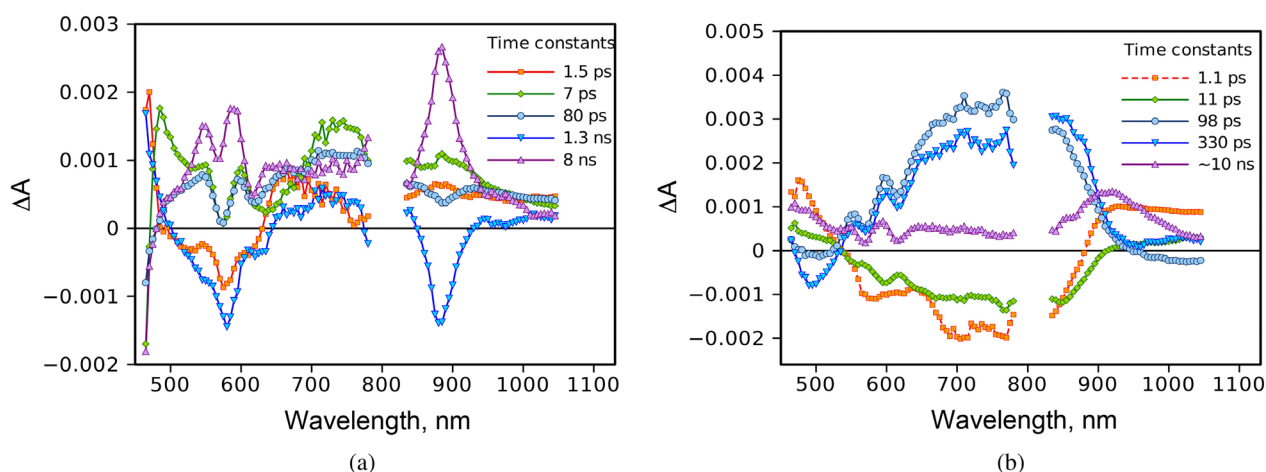


Fig. 10. Transient component spectra of T-P dyad in Hex (a) and AcCN (b) at  $\lambda_{\text{ex}} = 425$  nm

In acetonitrile (Fig. 9(b)) the two fast components correspond, as previously mentioned, to the singlet state decay (2.6 ps) of the porphyrin moiety and the simultaneous formation (19 ps) of the excited dyad, (T-P)\*. It has a broad absorption band from 600 nm to 910 nm and considerably shorter (350 ps) lifetime than in hexane. The final state is the charge transfer state with the absorption characteristic for porphyrin cation (600–800 nm) and that of the pyrene anion (870–950 nm).

The transient absorption component spectra, at 425 nm excitation, in hexane and acetonitrile are shown in Fig. 10. In hexane (Fig. 10(a)) the result shows a strong and broad absorption band with a lifetime of 7 ps and the maximum at *ca.* 750 nm, and clear bleaching of the ground state SnTPP absorption at 580 and 630 nm. This could correspond to the singlet excited state of the porphyrin. The next component, 80 ps, does not exist at 340 nm excitation, neither in fluorescence experiments. It has a very broad absorption band from the visible to the NIR region. That is followed by 1.3 ns and 8 ns components, which are similar to those observed with the 340 nm excitation, and assigned to the (T-P)\* state (1.3 ns) and the cation and anion radical (8 ns) of the SnTPP and pyrene moieties, respectively.

At 425 nm excitation (Fig. 10(b)) in AcCN the transient absorption responses are quite similar to those in hexane. A broad absorption with about 100 ps lifetime was not observed at the 340 nm excitation nor in the fluorescence experiments.

## FLUORESCENCE KINETICS

In the nonpolar solvent (hexane), independent of the excitation wavelengths, the fluorescence decays of the dyad at the porphyrin emission wavelength, can be analyzed as a single exponential decay with the time constant around 1.4–1.7 ns, which resembles that of

the porphyrin monomer [SnTPP(OH)<sub>2</sub>]. Moreover, the single component decay could also suggest that in a nonpolar solvent the excited state can be regarded as a state, in which the excitation is located in the porphyrin moiety, although the emission is red-shifted compared to that of SnTPP(OH)<sub>2</sub> and is less perturbed by the surrounding solvent molecules.

When the pyrene moiety is excited at 340 nm and monitored at the pyrene emission wavelength at 385 nm, the bi-exponential emission decay of the T-P dyad indicates an equilibrium between the excited ground state complex, (T-P)\*, and a newly formed excited complex between T and P. Energetically this is possible because the energy of the first excited state of pyrene is about the same as the energy of the Soret band of the porphyrin moiety. This is actually shown quite clearly in Fig. 5, where the decay of the fluorescence monitored at 385 nm is evidently bi-exponential with lifetimes of about 1 and 10 ns.

The dynamics when monitored at the pyrene emission wavelength could be described by an “equilibrium” kinetics as in Fig. 11.

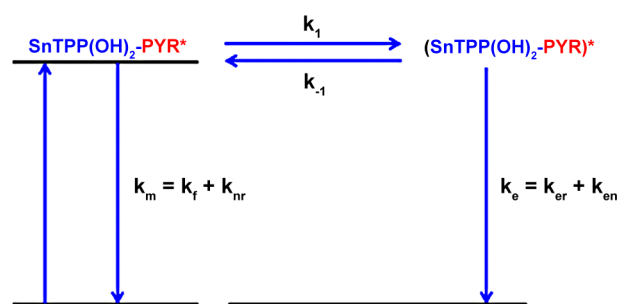


Fig. 11. The “equilibrium” dynamics when excited and monitored at the pyrene absorption and emission wavelengths, respectively

**Table 5.** Kinetic parameters calculated for **SnTPP(OH)<sub>2</sub>-PYR** monitored at pyrene emission.  $\lambda_{\text{ex}} = 340$  nm. All the rate constants are presented in  $\times 10^8 \text{ s}^{-1}$ 

Solvent	A <sub>1</sub>	A <sub>2</sub>	$\beta_1$	$\beta_2$	$k_m$	X	Y	$k_1[B]$	$k_{-1}$	$k_e$
Hexane	0.91	0.09	13.0	1.32	1.22	11.90	2.39	10.70	1.06	1.33
DCM	0.75	0.25	8.93	0.92	0.35	6.95	2.90	6.60	1.81	1.09
AcCN	0.86	0.14	10.6	0.97	0.66	9.31	2.30	8.65	1.28	1.02

By using the data in Table 3, the kinetic parameters in Fig. 11 could be calculated based upon Equations 3–5:

$$[A^*] = \frac{[A^*]_0}{\beta_1 - \beta_2} [(X - \beta_2)e^{-\beta_1 t} + (\beta_1 - X)e^{-\beta_2 t}] \quad (3)$$

$$[E^*] = \frac{k_1 [A^*]_0}{\beta_1 - \beta_2} [e^{-\beta_2 t} - e^{-\beta_1 t}] \quad (4)$$

$$\beta_{1,2} = \frac{1}{2} \left[ X + Y \mp \sqrt{(Y - X)^2 + 4k_1 k_{-1}} \right] \quad (5)$$

In Equations 3–5,  $X = k_m + k_1$  and  $Y = k_e + k_{-1}$ , where  $k_m$  is a relaxation rate (radiative + non-radiative) of the excited pyrene monomer, (T-P\*);  $k_1$  is the formation rate of the excited dyad,  $k_e$  and  $k_{-1}$  are the relaxation (radiative + non-radiative) rates of the excited dyad, (T-P)\*. The calculated kinetic parameters are presented in Table 5.

With the excitation at 405 nm, where the pyrene moiety absorbs significantly less than porphyrin, the time resolved fluorescence decays were also bi-exponential, but the longer-living components were 5–6 times shorter in time, 1.6–2.1 ns (Table 4), than those obtained by the **P** absorption and emission (Table 3). Thus the emission at >600 nm does not originate from the equilibrium state, which was formed and observed with the **P** excitation and emission, respectively. Also the relative amplitudes of the two emission bands (Fig. 4) at about 625 nm and 675 nm varied depending on solvent polarity and monitoring wavelength.

## MECHANISMS

The processes followed after the excitation of the T-P dyad can be described in all the solvents with practically the same mechanism (Fig. 12). First, when mainly the pyrene moiety in the T-P dyad is excited, the excitation is followed by an energy transfer to the porphyrin moiety. Then an excited dyad is formed and decays to a partial charge transfer complex, more efficiently in polar DCM and acetonitrile, than in nonpolar hexane. The existence of two different conformers and their influence on the ground and excited state properties of a porphyrin dimer linked by a vinylene spacer has been studied previously [18]. Thus, two possible conformers due to the vinyl chain, should be taken into account.

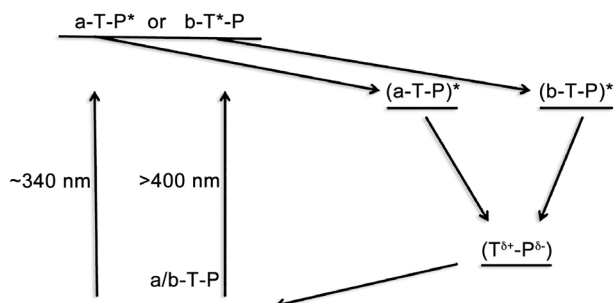


**Fig. 12.** The kinetic scheme for the decay processes followed the excitation of the pyrene moiety of the T-P dyad based on assumption on two conformers of the T-P dyad

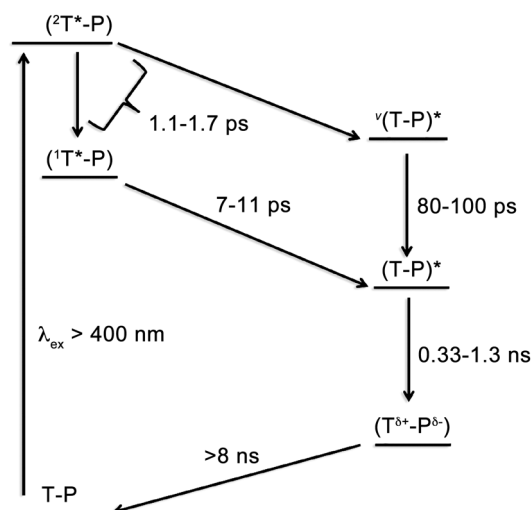


**Fig. 13.** The mechanisms at the 425 nm excitation. The scheme is based on the assumption on the electron transfer from the second excited state of porphyrin and the results of the pump-probe measurements shown in Fig. 10

Namely, two types of excited dyads, (a-T-P)\* and (b-T-P)\* are formed depending on the relative ground state concentration ratio of the conformers. The excited dyads have different lifetimes, from about 0.6 to 1.6 ns, depending on the environment. Finally the excited state dyads relax to charge transfer complexes and to the ground state.

Based on the time-resolved fluorescent (Figs 5 and 6) and pump-probe measurements (Figs 9 and 10) with

either pyrene or porphyrin excitation, it seems evident, that the mechanisms differ from each other at the very beginning of the photo-induced processes. The differences between 340 nm and 425 nm excitations can be qualitatively explained as follows (Fig. 13). The porphyrin excitation yields the excitation of the second excited state of porphyrin in the dyad, ( $^2T^*$ -P). This opens a possibility for an intramolecular charge transfer to occur from  $^2T^*$  state of the porphyrin to the pyrene moiety. This is quantitatively discussed by Mataga *et al.* [39] and recently by Fujitsuka *et al.* [40], and explains well the observed differences depending on the excitation wavelength. As the electron transfer would take place from the  $^2T^*$  state, it decays, in 1.1–1.7 ps (Fig. 10) to the  $^1T^*$  state, ( $^1T^*$ -P), and to an excited dyad, ( $^V(T-P)^*$ ). This state, which is not observed with the 340 nm excitation (Fig. 9), relaxes in 80–100 ps to a longer living excited dyad, ( $T-P)^*$ , which also is formed *via* the ( $^1T^*$ -P) state in 7–11 ps. ( $T-P)^*$  relaxes in 0.33–1.3 ns to the charge separated state, ( $T^{\delta+}$ - $P^{\delta-}$ ). The mechanism presented in Fig. 13 explains well the observation of five different component spectra in Fig. 10.

Analogically to the porphyrin excitation, the pyrene excitation (Fig. 9) could create an excited complex ( $^U(T-P)^*$ ) in few picosecond, which relaxes to the ( $T-P)^*$  state in 19–25 ps. The latter has lifetime 0.3–1.4 ns, depending on the solvent. The CT state formed after ( $T-P)^*$  has a lifetime >10 ns.

The properties of the transient states of ( $^V(T-P)^*$ ), ( $^U(T-P)^*$ ), and ( $T-P)^*$  resemble those known as intramolecular exciplexes, because they have emission bands, which differ from those of porphyrin or pyrene (Figs 4 and 8). The exciplexes, however, do not have fine structure, as the emission of the ( $T-P)^*$  state has two bands. This could be explained by the formations of two types of ( $T-P)^*$  states due to the different conformers [18] of the dyad in solution (Fig. 12). More intriguing explanation is, however, formation of different kinds of intramolecular exciplexes *via* the  $^1T^*$  and  $^2T^*$  states of the porphyrin moiety, as shown in Fig. 13.

## CONCLUSION

In conclusion, a Sn(IV)porphyrin-pyrene dyad has been synthesized showing photophysical behavior radically different from that of the constituent chromophores. Time-resolved fluorescence measurements show the existence of an intermediate emissive species, which is observed to be more stabilized in nonpolar hexane and shows a mono-exponential decay of 1.36 ns ( $\lambda_{ex}$  = 340 nm) or 1.52 ns ( $\lambda_{ex}$  = 425 nm), when observed at the porphyrin emission wavelength. Whereas, as the solvent polarity increases, a bi-exponential decay is observed with a variation in the component amplitudes, which could be due to the formation of charge separated state (CSS) as

an additional contributing species. However, from the pump-probe measurements, when excited at 425 nm, two different intermediate species are observed (~7–11 ps and 80–100 ps) with broad absorptions in the near-IR region, which imply the existence of two different conformers, which decays to the ground state *via* a CSS. An alternative explanation is that the intramolecular electron transfer and the formation of the final CSS state occurs *via* the second excited state of the porphyrin. The dyad synthesized serves as a molecular platform to demonstrate the influence of the flexible vinyl spacer on the excited state photophysics of the chromophores involved. Moreover, the presence of Sn(IV) metal center could assist in extending the axial coordination of the dyad molecules, further studies of which is in progress.

## Acknowledgements

HL acknowledges the financial support from the Academy of Finland (UVIADDEM) and the Finnish Funding Agency for Technology and Innovation (Biosphere). And LG acknowledges the Department of Science and Technology (DST, SB/S1/IC-14/2014) for financial support of this work.

## Supporting information

Figures S1–S8 and Tables 1–2 are given in the supplementary material. This material is available free of charge *via* the Internet at <http://www.worldscinet.com/jpp/jpp.shtml>.

## REFERENCES

1. *The Handbook of Porphyrin Science*, Kadish K, Smith K and Guillard R. (Eds.) World Scientific: Hackensack, NJ, 2010.
2. Imahori H, Umeyama T and Ito S. *Acc. Chem. Res.* 2009; **42**: 1809–1818.
3. Campbell WM, Burrell AK, Officer DL and Jolley KW. *Coord. Chem. Rev.* 2004; **248**: 1363–1369.
4. Walter MG, Rudine AB and Wamser CC. *J. Porphyrins Phthalocyanines* 2010; **14**: 759–792.
5. Perez MD, Borek C, Forrest SR and Thompson ME. *J. Am. Chem. Soc.* 2009; **131**: 9281–9286.
6. Kira A, Matsubara Y, Iijima H, Umeyama T, Matano Y, Ito S, Niemi M, Tkachenko NV, Lemmetyinen H and Imahori H. *J. Phys. Chem. C* 2010; **114**: 11293–11304.
7. Baldo MA, O' Brien DF, You Y, Shoustikov A, Sibley S, Thompson ME and Forrest SR. *Nature* 1998; **395**: 151–154.
8. Murphy AR and Fréchet JM. *Chem. Rev.* 2007; **107**: 1066–1096.
9. McConnell I, Li G and Brudvig GW. *Chem. Biol.* 2010; **17**: 434–447.

10. Gust D, Moore TA and Moore AL. *Acc. Chem. Rev.* 2009; **42**: 1890–1898.
11. Liu JY, El-Khouly ME, Fukuzumi S and Ng DKP. *Chem. Eur. J.* 2011; **17**: 1605–1613.
12. Aratani N, Kim D and Osuka A. *Acc. Chem. Res.* 2009; **42**: 1922–1934.
13. Albinsson B and Mårtensson J. *J. Photochem. Photobiol. C: Photochem. Rev.* 2008; **9**: 138–155.
14. Aratani N, Cho HY, Ahn TK, Cho S, Kim D, Sumi H and Osuka A. *J. Am. Chem. Soc.* 2003; **125**: 9668–9681.
15. Tsuda A, Nakamura Y and Osuka A. *Chem. Commun.* 2003; **9**: 1096–1097.
16. Osuka A, Tanabe N, Nakajima S and Maruyama K. *J. Chem. Soc. Perkin Trans.* 1996; **2**: 199–204.
17. Susumu K, Shimidzu T, Tanaka K and Segawa H. *Tetrahedron Lett.* 1996; **37**: 8399–8402.
18. Chachisvilis M, Chirvony VS, Shulga AM, Källebring B, Larsson S and Sundström V. *J. Phys. Chem.* 1996; **100**: 13867–13873.
19. Flamigni L, Johnston MR and Giribabu L. *Chem. Eur. J.* 2002; **8**: 3938–3947.
20. Bonfantini EE, Burrell AK, Campbell WM, Crossley MJ, Gosper JJ, Harding MM, Officer DL and Reid DCW. *J. Porphyrins Phthalocyanines* 2002; **6**: 708–719.
21. Ventura B, Barigelletti F, Lodato F, Officer DL and Flamigni L. *Phys. Chem. Chem. Phys.* 2009; **11**: 2166–2176.
22. Bonfantini EE, Burrell AK, Officer DL and Reid DCW. *Inorg. Chem.* 1997; **36**: 6270–6278.
23. Lembo A, Tagliatesta P and Guild DM. *J. Phys. Chem. A* 2006; **110**: 11424–11434.
24. Reeta PS, Ravikumar K and Giribabu L. *J. Chem. Sci.* 2013; **125**: 259–266.
25. Kandhadi J, Kanaparthi RK and Giribabu L. *J. Porphyrins Phthalocyanines* 2012; **16**: 282–289.
26. Vijendra SS and Mangalampalli R. *Inorg. Chem.* 2011; **50**: 1713–1722.
27. Giribabu L, Kumar CV and Reddy PY. *Chem. Asian J* 2007; **2**: 1574–1580.
28. Giribabu L, Kumar CV and Reddy PY. *J. Porphyrins Phthalocyanines* 2006; **10**: 1007–1016.
29. Arnold DP and Janet B. *Coord. Chem. Rev.* 2004; **248**: 299–319.
30. Poddutoori PK, Zarrabi N, Moiseev AG, Brisa RG, Vassiliev S and Van der Est A. *Chem. Eur. J.* 2013; **19**: 3148–3161.
31. Giribabu L, Ashok Kumar A, Neeraja V and Maiya BG. *Angew. Chem. Int. Ed.* 2001; **40**: 3621–3624.
32. Perrin DD, Armarego WLF and Perrin DR. *Purification of Laboratory Chemicals*, Oxford: Pergamon, 1986.
33. Kesti TJ, Tkachenko NV, Vehmanen V, Yamada H, Imahori H, Fukuzumi S and Lemmetyinen H. *J. Am. Chem. Soc.* 2002; **124**: 8067–8077.
34. Tkachenko NV, Rantala L, Tauber AY, Helaja J, Hynninen PH and Lemmetyinen H. *J. Am. Chem. Soc.* 1999; **121**: 9378–9387.
35. Stranius K, Iashin V, Nikkonen T, Muuronen M, Helaja J and Tkachenko NV. *J. Phys. Chem. A* 2014; **118**: 1420–1429.
36. Kadish KM, Xu QY, Maiya GB, Barbe J-M and Guillard R. *J. Chem. Soc., Dalton Trans.* 1989; **8**: 1531–1536.
37. Berezovskii VV, Wöhrle D, Tsaryova O, Makarov SG, Pomogailo SI, Glagolev NN, Zhilina ZI, Voloshanovskii IS, Roshchupkin VP and Pomogailo AD. *Russ. Chem. Bull. Int. Ed.* 2007; **56**: 160–167.
38. Reddy RD and Maiya BG. *J. Porphyrins Phthalocyanines* 2002; **6**: 3–11.
39. Mataga N, Taniguchi S, Chosrowjan H, Osuka A and Yoshida N. *Chem. Phys.* 2003; **295**: 215–228.
40. Fujitsuka M, Shiragami T, Cho DW, Tojo S, Yasuda M and Majima T. *J. Phys. Chem. A* 2014; **118**: 3926–3933.